2020 8th IEEE International Conference on Biomedical
Robotics and Biomechatronics (BioRob)
New York, USA. Nov 29 - Dec 1, 2020

Development of Haptic Approaches for a Head-Controlled Soft Robotic Endoscope

Y. X. Mak[†1], A. Lanciano[†2], S. Stramigioli[1], and M. Abayazid[1]

***Abstract*— Recent advances in soft robotics are utilized to solve challenges in endoscopy, such as maneuverability, flexibility, and the structural stiffness required to deliver enough force during endoscopic surgical procedure. Other major challenge is the lack of haptic feedback from the tool end-effector to the surgeon. Current clinical practice in minimally invasive intervention requires an assistant to control the camera since the surgeon is preoccupied with task at hand, creating a indirect control procedure for maneuvering the endoscope. For the soft robotic endoscope, we implemented a haptic feedback interface along with a novel control method to concurrently tackle these challenges. The user of the developed system can visualise the planned 2D insertion path and steer the endoscope module accordingly using an inertial measurement unit mounted on a head-band. Furthermore, five different haptic feedback methods (three kinesthetic and two vibrotactile) were compared in term of user accuracy while steering the endoscope along a planned path. The results show that the user's accuracy using kinesthetic and vibrotactile feedback were comparable, however, participants of this study find vibrotactile feedback approach more preferable for its intuitiveness and comfort.**

I. Introduction

Minimally invasive surgery (MIS) are gradually replacing conventional open surgery due to its benefits, such as reduced patient's trauma and recovery duration. However, there are limitations in MIS procedures caused by the lack of surgical tool's flexibility to safely maneuver and reach difficult targets. A more flexible endoscopic toolkit opens up more minimally invasive procedure possibilities, such as deeper surgical reach in Transanal endoscopic operation (TEO) procedures. On the contrary, the tool also has to be stiff enough to push the endoscope forward and deliver enough force during the procedure, such as during biopsy procedure using colonoscope. This creates a paradoxical problem of the endoscope has to be stiff and compliant simultaneously [1].

Another problem that needs to be solved in using flexible endoscope is the lack of haptic feedback to the user. A study conducted by Wagner et al. [2] indicates that absence of haptic feedback increases the magnitude of force applied to tissue by at least 50%, and increases the number of tissue damaging errors by more than three times [3]. This has been considered as one of the major limitation in using flexible tools for MIS.

Haptic feedback can be used to deliver tactile sensing based on the real-time signal from the tip of endoscope, or to give guidance to surgeons in order to follow a pre-planned path. For the latter case, the technique is also called *haptic virtual fixtures* [4]. This approach is categorized into two main methods: Guidance Virtual Fixtures (GVF) and Forbidden-region Virtual Fixtures (FRVF) [5]. The aim of these methods is to help surgeons to perform robot-assisted manipulation tasks, by guiding the surgeon along a desired path and limiting their movements against restricted and sensitive regions.

Haptic feedback can be separated into two categories [6]: *kinesthetic* (related to forces and positions) and *cutaneous* (related to the skin, tactile). In recent development related to surgical tools, the use of *non-kinesthetic* haptic feedback becomes more widespread through alternative forms of feedback such as vibrotactile [7]-[9] and skin-stretch devices.

Looking into other limitations in MIS, a better control method is needed to reduce the dependencies on the communication between surgeon and the assistant who controls the endoscope during an intervention. Several solutions had been proposed to move the control from the assistant to the surgeon directly, such as single-hand controlled [10], body controlled [11], eye-movement controlled [12], image-guided [13][14], and lastly a head-controlled endoscope system, [15] which is relevant to the control approach used in this study.

With the recent development of soft robotics endoscope systems, several groups tried to combine the different needs of MIS into a single robotic system. A soft endoscopic system developed by Cianchetti et al. called STIFF-FLOP [16]-[17] uses pneumatic actuation. Other soft endoscopes have been designed using different actuation mechanism, such as MINIR [18] using shape-memory-alloy mechanism, and Meshworm designed by Bernth et al. [19] that is actuated using tendon cables. Based on the STIFF-FLOP approach, a new concept with four inner chambers has been developed by Naghibi et al. [20] [21], called MOLLUSC. Our research work uses the previously developed MOLLUSC design which has 2 degrees of freedom (DOF) bending capability through pressurization of antagonistic chambers.

Therefore, in order to address the challenges in MIS, the novelty of this study lies in:

- Development of a head-motion controlled soft robotic endoscope system such that the surgeon can control the endoscope directly without the help of a camera-

[†]Y. X. Mak and A. Lanciano contributed equally towards the results of this paper

This work is financially supported by ITEA-3 funding organization under 17021 IMPACT project.

[1]Y. X. Mak, S. Stramigioli, and M. Abayazid are with Robotics and Mechatronics group, Faculty of Electrical Engineering, Mathematics and Computer Science, Technical Medicine Centre, University of Twente, 7500 AE Enschede, the Netherlands

[2]A. Lanciano is affiliated with the Department of Electrical Engineering and Information Technology, Universita degli Studi di Napoli Federico II 80125 Napoli, Italy.

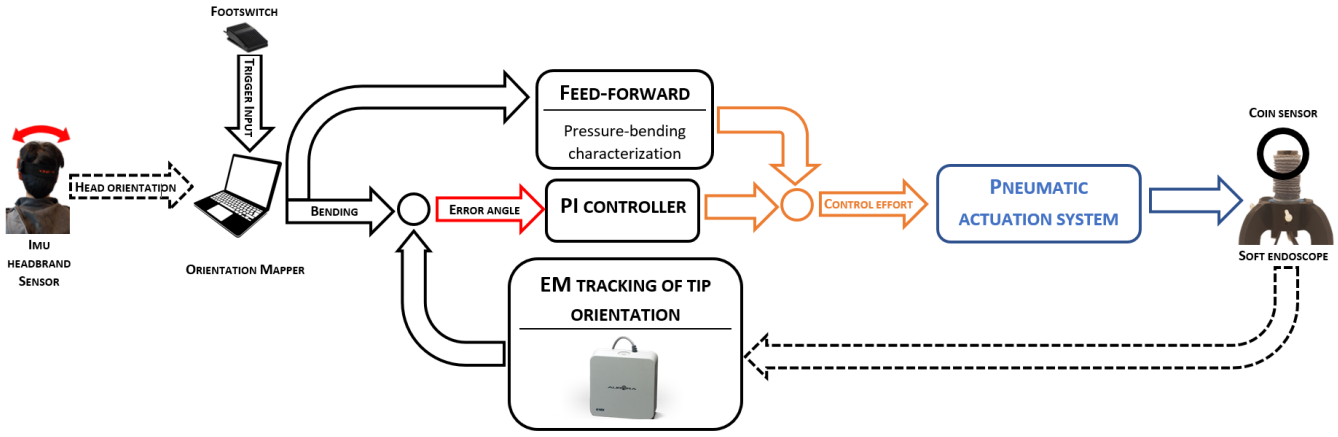

Fig. 1. Control structure of the head-motion controlled soft robotic endoscope system.

assistant.

- Human-in-the-loop experimental evaluation of various haptic approaches for guiding the clinicians to follow a planned trajectory.

II. Materials and Methods

A. Head Orientation Tracking

The aim of this study is to control the tip bending of the endoscope using the clinician's head motion, which can be implemented in several ways, such as using optical markers, distance sensor, electromagnetic tracker, inertial sensors, etc. We opted to use a wireless Inertial Measurement Unit (IMU) tracker, which consist of an accelerometer, gyroscope, and magnetometer to track the head orientation. IMU is chosen due to its simplicity and it does not require direct line-of-sight such as in the case of optical trackers, which is not always feasible in an operating room.

Furthermore, to let the clinicians move their head freely when they do not need to control the endoscope tip movement, the system is equipped with a foot-switch in order to implement a trigger mechanism that enable and disable the endoscope control. This orientation mapper block, as presented in Fig. 1 consists of 3 components:

1) Orientation mapping from head to endoscope tip: Since the orientation output from the IMU sensor is given as current IMU orientation compared to the earth magnetic field orientation, a transformation between IMU frame to head frame is needed. Hence, the orientation of the user's head is given as:

$$\mathbf{q}_e^h = \mathbf{q}_{\text{IMU}}^h \odot \mathbf{q}_e^{\text{IMU}} \tag{1}$$

where $\odot$ denotes a quaternion multiplication operator, $\mathbf{q}_{\text{IMU}}^h \in \text{SU}(2)$ is the transformation from IMU frame to the head frame, and $\mathbf{q}_e^{\text{IMU}} \in \text{SU}(2)$ is the orientation output from the IMU sensor.

2) Saving the orientation from previous foot-switch session: The idea is to have a position-based mapping [12], between the head and endoscope tip, where the mapping is continuous between foot-switch 'session', i.e., the last orientation when the foot-switch was released equals the orientation when the foot-switch is re-pressed. This will enable the user to move without workspace restriction, analogous to the movement of a computer mouse. Thus, for a head frame $h_{s,k}$ in session s at time instance t, the head orientation can be calculated by:

$$\mathbf{q}_{h_{1,1}}^{h_{s,t}} = \mathbf{q}_{h_{s,1}}^{h_{s,t}} \odot \mathbf{q}_{h_{s-1,1}}^{h_{s-1,\text{end}}} \odot \cdots \odot \mathbf{q}_{h_{1,1}}^{h_{1,\text{end}}} . \tag{2}$$

This can be simplified by saving the head orientation from the end of previous session:

$$\mathbf{q}(s,t) = \mathbf{q}_{h_{s,1}}^{h_{s,t}} \odot \mathbf{q}(s-1, t_{s-1,\text{end}}) . \tag{3}$$

3) Scaling between head and endoscope movement: In order to control the tip of the endoscope with more accuracy, the mapping between head to endoscope tip can be scaled linearly using Spherical Linear Interpolation (SLERP) [22] between an identity quaternion $\mathbf{q}_I$ and orientation change in the current session $\mathbf{q}_{h_{s,1}}^{h_{s,t}}$:

$$\mathbf{q}_{\text{scaled}}(s,t) = \text{slerp}\left(\mathbf{q}_I, \mathbf{q}_{h_{s,1}}^{h_{s,t}}\right) \odot \mathbf{q}(s-1, t_{s-1,\text{end}}) . \tag{4}$$

B. Control

A control system was implemented to control the bending angle θ of the tip of the endoscope.

1) Feed-forward / open-loop control: The feed-forward control block (in Fig. 1) contains the pressure-angle static characterization of the soft endoscope modules. Since the endoscope consists in four chambers with quite different response due to manufacturing inconsistencies, we took the mean of the characterizations, given in Fig. 2. The centerline of the hysteresis loop is fitted using spline curve which is used in the feed-forward signal calculation.

2) Closed-loop control: The closed-loop controller structure Figure 1, the total control effort consists of two contributions: (1) open-loop pressure value based from a priori knowledge, and (2) closed-loop pressure effort value provided by the computation through a Proportional-Integral (PI) Controller.

Hence, the pressure to be applied to the actuators (chambers) is computed by a linear process that takes the current

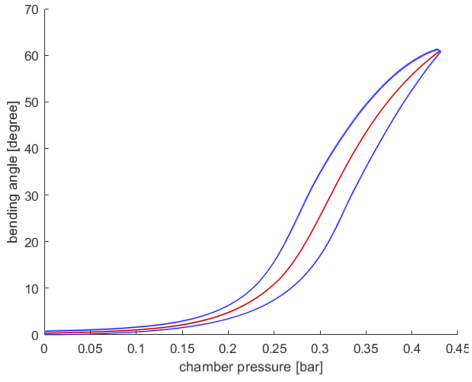

Fig. 2. Characteristic pressure to endoscope tip bending relation (blue) for the MOLLUSC soft endoscope module identified by applying increasing and decreasing input pressure. The center-line (red) of the average hysteresis loop over 4 chambers is used in the feed-forward signal.

control effort value, selects the right actuator to be activated and sends the control effort value to the Arduino where the pneumatic motors are connected.

C. Path planning

For the purpose of assessing the virtual fixture haptic feedback, we require a reference trajectory, simulating an optimal path for endoscopic insertion. We defined two main requirements for the path planning algorithm:

1) Prescribed waypoints: keypoints in 2D plane which the endoscope has to pass, should be chosen a priori before the insertion procedure.
2) Smooth path: the path has to be smooth in order to avoid sharp turns which the endoscope may not be able to follow.

Therefore, we focused on a smooth path planning algorithm and implemented an algorithm based on Bezier splines connecting the waypoints defined manually by the user [23]. The cubic splines curve $\mathbf{x}_i$ parametrized by length u between two waypoints $\mathbf{P}_i$ and $\mathbf{P}_{i+1}$ is given by:

$$\begin{aligned}\mathbf{x}_i(u) = &\left(2\frac{(u-u_i)^3}{(\Delta u_i)^3} - 3\frac{(u-u_i)^2}{(\Delta u_i)^2} + 1\right)\mathbf{P}_i + \\ &+\left(-2\frac{(u-u_i)^3}{(\Delta u_i)^3} + 3\frac{(u-u_i)^2}{(\Delta u_i)^2} + 1\right)\mathbf{P}_{i+1} + \\ &+\left(\frac{(u-u_i)^3}{(\Delta u_i)^2} - 2\frac{(u-u_i)^2}{(\Delta u_i)} + u - u_i\right)\mathbf{P}'_i + \\ &+\left(\frac{(u-u_i)^3}{(\Delta u_i)^2} - \frac{(u-u_i)^2}{(\Delta u_i)}\right)\mathbf{P}'_{i+1}\end{aligned} \tag{5}$$

where $\mathbf{P}_i$ and $\mathbf{P}_{i+1}$ are two generic neighboring waypoints while $\mathbf{P}'_i$ and $\mathbf{P}'_{i+1}$ are the corresponding derivatives defined as: $\mathbf{x}_i(u_i) = \mathbf{P}_i$, $\mathbf{x}_i(u_{i+1}) = \mathbf{P}_{i+1}$, $\mathbf{x}'_i(u_i) = \mathbf{P}'_i$ and $\mathbf{x}'_i(u_{i+1}) = \mathbf{P}'_{i+1}$.

Fig. 3 shows a synthetic colon image used to imitate CT scan 2D slice (coronal plane) of patient's colon, along with the generated path. This trajectory will be used to validate the accuracy of each haptic feedback methods in Section III.

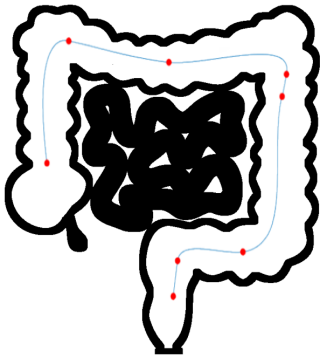

Fig. 3. Synthetic 2D slice (coronal plane) of patient's colon with prescribed waypoints and the generated endoscope insertion path

D. Haptic Feedback Methods

Using the virtual fixtures approach, particularly the Guidance Virtual Fixtures (GVF), several different kinesthetic and non-kinesthetic feedback methods can be employed. With haptic feedback, users are provided with guiding information based the difference between their current position and the simulated optimal trajectory.

Non-kinesthetic feedback is a type of haptic feedback that does not include dynamic aspects of haptic interaction, or in other words, interaction which does not involve 'dynamic' motion or force. In this work we are focusing on two vibrotactile feedback methods: using 2 vibration motors to relay information based on signal amplitude, and relaying information using both amplitude and frequency of vibration using only 1 vibration motor.

1) Vibration feedback with two motors (FB1): Two vibration motors are placed, one each on the back of of user's hand to accommodate control of other tools during procedure which will occupy the surgeon's hands (see Fig. 4).

The output signals given to the vibration motors are based on the difference between the optimal orientation $\theta_{\text{ref}}(t)$ and the current orientation $\theta(t)$ of the endoscope along the path:

$$f_v = A\left(\theta_{\text{ref}}(t) - \theta(t)\right) , \tag{6}$$

where A is an amplitude scaling chosen to set the just-noticeable difference at small error angle. Two vibration motors are used in order to provide the direction of the error, and the vibration amplitude of each motor provides how much the user should bend their head to that side. When user does not feel any vibrations on both hands, the desired reference bending is reached.

2) Vibration feedback with one motor (FB2): This method is similar to the one presented in [8], however, only one vibration motor is used at the back of user's hand (see Figure 4). In this case, the direction of the error is signaled using different vibration frequencies:

$$f_v = A\left|\theta_{\text{ref}}(t) - \theta(t)\right| \operatorname{sgn}(\sin(2\pi f t)) , \tag{7}$$

$$\text{where } f = \begin{cases} 100\text{Hz} & \text{if } (\theta_{\text{ref}} - \theta) > 0 \\ 25\text{Hz} & \text{if } (\theta_{\text{ref}} - \theta) \leq 0 \end{cases}$$

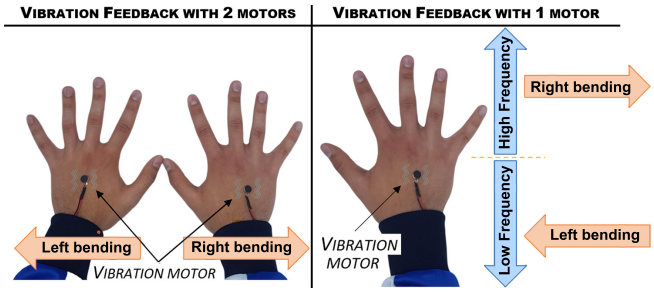

Fig. 4. Vibrotactile feedback with 2 motors (FB1, left image) and with 1 motor (FB2, right image)

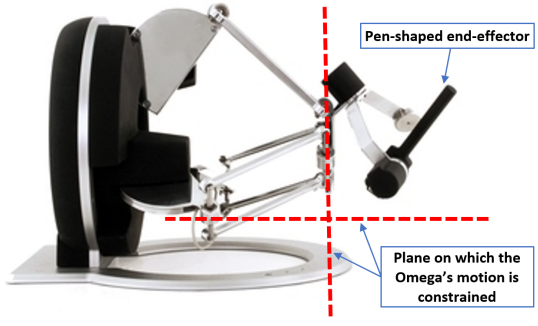

Fig. 5. Side view of the omega.6 haptic device, used for force (FB3), position (FB4), and virtual wall boundary feedback (FB5) method.

Hence, the vibration amplitude provides information about how far/close you are from the optimal bending angle, while vibration frequency signals the direction of the bending error. When user does not feel any vibrations, the desired reference bending is reached.

Using *kinesthetic feedback*, users are equipped with a haptic feedback device which will provide motion or force interaction. Omega.6 haptic device (Force Dimension, Switzerland) is used in this study. Since the haptic signal to the user only conveys 1 degree of freedom movement, we defined two orthogonal planes on which the pen's motion are constrained to (see Fig. 5).

3) Force feedback (FB3): In this haptic feedback method, the device will exert force to the user's hand in the direction of the error, which is the difference between the optimal orientation $\theta_{\text{ref}}(t)$ and the current orientation $\theta(t)$ of the endoscope along the path.

$$f_y = A\left(\theta_{\text{ref}}(t) - \theta(t)\right) . \tag{8}$$

When user does not feel any force feedback, the reference bending is reached.

4) Position feedback (FB4): This method specifies a linear spring model which pulls the pen-shaped end-effector in the direction/location of the target position $p_{y,\text{ref}}$, that is dependent on the bending error. It is expressed by the following equation:

$$f_y = K\left(p_{y,\text{ref}} - p_y\right) \tag{9}$$

where f_y is the haptic force feedback (i.e., the force applied to the omega.6 pen), p_y is the position of the haptic pen and

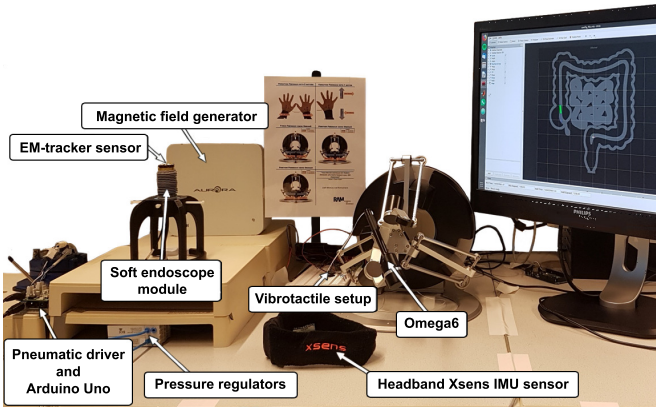

Fig. 6. Experimental setup for the head-controlled soft robotic endoscope system validation.

$p_{y,\text{ref}}$ is the target position of the pen based on the bending error. Equation (9) represents a linear spring with stiffness K and it has an equilibrium point at $p_y = p_{y,\text{ref}}$. When the equilibrium is at the center of the device, i.e., $p_y = p_{y,\text{ref}} = 0$, the user would know that the reference bending is reached.

5) Virtual wall feedback (FB5): Using the idea of Forbidden-region Virtual Fixtures (FRVF), we implemented two 'virtual walls' which location will change depending on the bending error direction and amplitude. During operation, user will feel the '*free space*' in the direction of the bending error. When the user cannot move the omega.6's pen, the reference bending is reached.

III. Validation

In this section, the accuracy performance of the controller is validated. Furthermore, to compare human-in-the-loop accuracy performance of the haptic feedback methods, endoscope insertion experiments were conducted.

A. Experimental setup

The physical setup is shown in Figure 6, where different system modules are shown.

In term of physical setup, the head-controlled soft robotic endoscope system can be categorized into five subsystems:

1) Head-motion controller, which consists of an IMU tracker, foot-switch, and the mapping algorithm between the head and endoscope tip.
2) Haptic feedback device, using omega.6 haptic device and vibration motors
3) Visualization of the endoscope moving along the generated path on a monitor, using Robot Operating System (ROS) framework
4) Soft robotic endoscope module
5) Pneumatic actuation system

Particularly, the head-motion controller subsystem consists of two devices, the wireless IMU sensor MTw Awinda (Xsens Technologies B.V., the Netherlands) and a foot-switch, which aim was explained in Sec. II-A. A computer screen is necessary to show the path visualization, letting the

experiment participants see the endoscope module moving along the generated reference path (see Sec. II-C)

The endoscope used for this experiment is a soft pneumatic endoscope module [21], with 4 pneumatic chambers and external sheath to constrain the chamber expansion in radial direction. A pneumatic actuation system which consists of an Arduino with a pneumatic driver shield [24] is connected to two pressure regulators (Festo AG & Co. KG) running on 2 bar pressure source.

B. Controller accuracy validation

To assess the accuracy performance of the closed loop controller, we measured the system dynamic response of the open and closed loop controllers, using step and ramp reference signal.

The open loop controller is based on the pressure-bending characteristic curve of the soft endoscope, while the closed-loop controller includes both PI feedback controller and the characteristic curve. The step reference signal is defined as $0°$ to $30°$ step at $t = 0$ for both side of the bending. The ramp reference signal goes from $0°$ to $60°$ over 100 seconds with $0.01°$ of resolution at 10 Hz.

C. Haptic feedback evaluation

In the endoscope insertion experiment, participants were asked to steer the endoscope module such that the tip position aligns with the reference insertion path.

1) Experiment design: The base of the module prescribed to move at a constant speed of 2 cm/s along the reference path. The bending error is defined as the difference between tip orientation (provided by the user), to the optimal bending orientation that minimizes the error of endoscope's tip position to the path. For this validation experiment, we used the closed-loop controller with module characteristic curve feed-forward. This experiment is conducted for each haptic feedback methods outlined in Sec. II-D.

Before the test, participants were asked to perform one training insertion experiment using a different reference path, to familiarize themself with the task. The reference insertion path used in the insertion experiment is shown in Fig. 3. During the experiments, the participants are allowed to see both the physical module and the visualization at the monitor, along with the guidance from each haptic feedback method. Afterwards, the participants were asked to fill out a questionnaire form, to get feedback regarding their user experience in using the head-controlled endoscope system with different haptic feedback methods.

2) Participants: A total of fourteen participants performed the experiment (3 females and 11 males, age 24-32). Five participants were technical medicine MSc students who had completed a training in clinical insertions and endoscopy. Additionally, five PhD student participants who are currently working on endoscopy field and four biomedical engineers were enrolled to participate in the experiments.

The subjects participated in the experiments on voluntary basis and signed an informed consent. The participants were informed about the procedure before the beginning of the experiment.

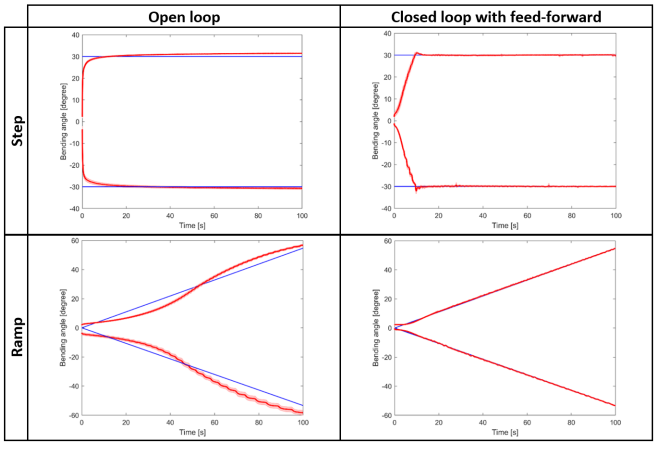

Fig. 7. Measured planar tip orientation (red) given two kinds of reference input (blue). Two kinds of input references are given, step signal (top images) and ramp signal (bottom images). A maximum velocity threshold value is prescribed to the system to avoid instability problem with the step reference input.

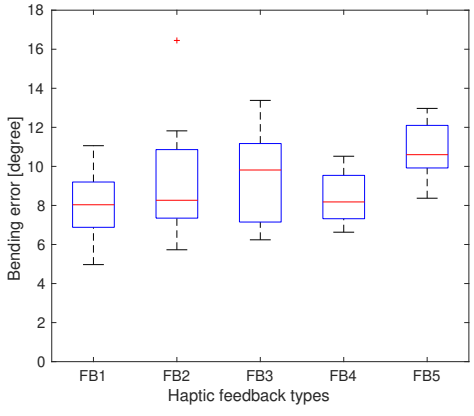

Fig. 8. Distribution of RMSE by the subject participants for different haptic feedback methods in the insertion experiment.

The bending error for each haptic feedback method for all subject participants were compared using one-way analysis of variance (ANOVA) to check whether there are statistical differences in human-in-the-loop accuracy performance between the haptic feedback methods. Significance level $\alpha = 0.05$ in this statistical test.

IV. Results and Discussion

A. Controller accuracy

Fig. 7 shows the response of the open-loop and closed-loop controller for different reference signals. In open-loop mode, there is inaccuracy around $0°$ for the ramp signal since the endoscope module has a dead-zone between 0 to 0.2 bar as indicated in Fig. 2. The closed-loop controller (as shown in Fig. 7) has a more accurate response for both step and ramp reference signals compared to the open-loop controller.

	Questions	Vibration feedback with 2 motors	Vibration feedback with 1 motor	Force feedback	Position feedback	Virtual wall feedback
Q1	The most intuitive feedback was:	71 %	7 %	0 %	7 %	14 %
Q2	The most comfortable feedback was:	71 %	0 %	7 %	21 %	0 %
Q3	I felt more tired with:	0 %	7 %	14 %	14 %	64 %
Q4	The most helpful feedback to figure out the side was:	64 %	0 %	29 %	0 %	7 %
Q5	The feedback that helped me more to reach the right point was:	64 %	0 %	7 %	14 %	14 %

TABLE I

SUBJECT PARTICIPANTS WERE ASKED TO POINT OUT WHICH HAPTIC FEEDBACK METHOD CORRESPONDS THE MOST WITH THE GIVEN STATEMENTS.

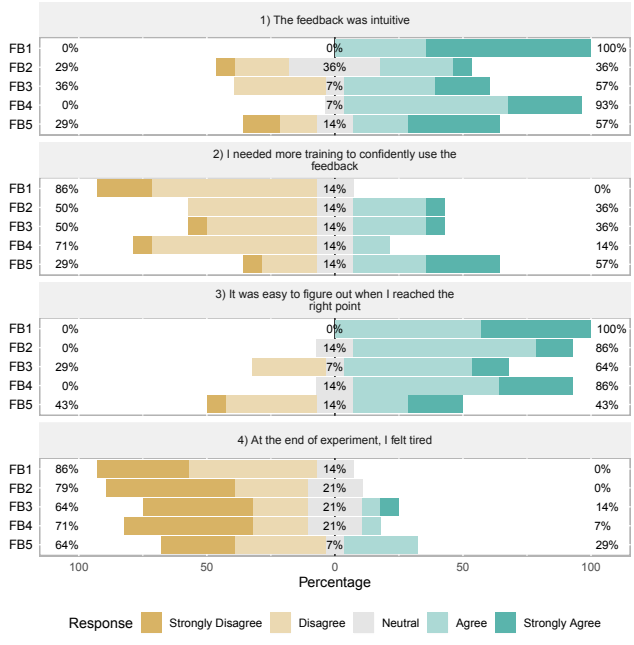

Fig. 9. Response for the questionnaires regarding user experience for different haptic feedback methods.

B. Haptic feedback comparison

In order to evaluate human accuracy when using the head-controlled soft robotic endoscope system, we recorded the bending error for each participant measured over the entire reference path during the insertion experiments. Then, the Root Mean Square Error (RMSE) for the whole trajectory was calculated for each participant and each haptic feedback method. Fig. 8 shows the error distribution from the collected data for the five different feedback experiments over all subject participants in a boxplot chart.

A one-way ANOVA statistical analysis showed a statistically significant difference between the means of 'vibration feedback with 2 motors' and 'virtual wall feedback' method ($p = 0.003$). Furthermore, it also showed a statistically significant difference between the means of 'position feedback' and 'virtual wall feedback' method ($p = 0.024$).

C. Questionnaire results

Right after the experiment, we asked the participants fill out a questionnaire concerning their experience in using different haptic feedback methods in the insertion experiment. Participants were required to rate statements given in the questionnaire from 'strongly disagree' to 'strongly agree'. The results are shown in Fig. 9.

Moreover, the participants were asked to give a general point of view by choosing the preferred feedback method. The result is shown in Table IV-B, where the majority of experiment participants stated 'vibration feedback with 2 motors' is more intuitive and comfortable compared to other type of haptic feedback methods. The results suggest that there is a trade-off between intuitiveness and the information complexity which is being conveyed by the haptic signal. Based on observation during the experiment, participants favoured the vibration feedback method due to the familiarity that they have with these kind of cues instead of dynamic motion cues, leading to a more intuitive experience.

V. CONCLUSION

In this study, a head-motion controlled soft robotic endoscope has been developed and a closed-loop controller has been successfully implemented, satisfying the accuracy requirement for endoscopic steering application. Moreover, a path planning algorithm was implemented to generate endoscope insertion path, which simulates the desired insertion trajectory known prior to the insertion procedure.

Five different haptic feedback methods were compared in term of user accuracy performance in controlling the endoscope along a 2D insertion path. Participants of the insertion experiment were able to perform the experiments more accurately using vibration feedback haptic feedback with 2 motors on each hand. While, using virtual wall feedback method, experiment participants showed highest inaccuracy in tracing the reference path, compared to the other haptic feedback methods. According to the questionnaire results, the vibrotactile feedback which uses 2 motors to signal the error magnitude and direction was the preferred haptic feedback in terms of intuitiveness and comfort. More broadly, additional system development such as stacking, downsizing, and developing control algorithm for multi-segment soft robotic endoscope is required to progress towards a clinical application. A further study with clinician participants is required to ensure information regarding endoscope shape and position is delivered in the most effective manner, as the proposed approach relies on proper visualization of the robot in conjunction with the haptic feedback.

REFERENCES

[1] A. Loeve, P. Breedveld, and J. Dankelman, "Scopes Too Flexible...and Too Stiff," *IEEE Pulse*, vol. 1, no. 3, pp. 26–41, Nov. 2010.

[2] C. R. Wagner, N. Stylopoulos, and R. D. Howe, "The role of force feedback in surgery: analysis of blunt dissection," in *Proceedings 10th Symposium on Haptic Interfaces for Virtual Environment and Teleoperator Systems. HAPTICS 2002*. Citeseer, 2002, pp. 68–74.

[3] C. R. Wagner, N. Stylopoulos, P. G. Jackson, and R. D. Howe, "The benefit of force feedback in surgery: Examination of blunt dissection," *Presence: teleoperators and virtual environments*, vol. 16, no. 3, pp. 252–262, 2007.

[4] N. Turro and O. Khatib, "Haptically augmented teleoperation," in *Experimental Robotics VII*. Springer, 2001, pp. 1–10.

[5] J. J. Abbott, P. Marayong, and A. M. Okamura, "Haptic virtual fixtures for robot-assisted manipulation," in *Robotics research*. Springer, 2007, pp. 49–64.

[6] A. M. Okamura, "Haptic feedback in robot-assisted minimally invasive surgery," *Current opinion in urology*, vol. 19, no. 1, p. 102, 2009.

[7] R. E. Schoonmaker and C. G. Cao, "Vibrotactile force feedback system for minimally invasive surgical procedures," in *2006 IEEE international conference on systems, man and cybernetics*, vol. 3. IEEE, 2006, pp. 2464–2469.

[8] M. Abayazid, C. Pacchierotti, P. Moreira, R. Alterovitz, D. Prattichizzo, and S. Misra, "Experimental evaluation of co-manipulated ultrasound-guided flexible needle steering," *The International Journal of Medical Robotics and Computer Assisted Surgery*, vol. 12, no. 2, pp. 219–230, 2016.

[9] C. Pacchierotti, M. Abayazid, S. Misra, and D. Prattichizzo, "Teleoperation of steerable flexible needles by combining kinesthetic and vibratory feedback," *IEEE transactions on haptics*, vol. 7, no. 4, pp. 551–556, 2014.

[10] E. D. Rozeboom, J. G. Ruiter, M. Franken, M. P. Schwartz, S. Stramigioli, and I. A. Broeders, "Single-handed controller reduces the workload of flexible endoscopy," *Journal of robotic surgery*, vol. 8, no. 4, pp. 319–324, 2014.

[11] A. M. Martinez, J. V. Gomez, R. O. Flores, and D. L. Espinoza, "Postural mechatronic assistant for laparoscopic solo surgery (pmass)," *Surgical endoscopy*, vol. 23, no. 3, p. 663, 2009.

[12] G. P. Mylonas, A. Darzi, and G. Z. Yang, "Gaze-contingent control for minimally invasive robotic surgery," *Computer Aided Surgery*, vol. 11, no. 5, pp. 256–266, Jan. 2006. [Online]. Available: https://doi.org/10.3109/10929080600971344

[13] N. van der Stap, L. Voskuilen, G. de Jong, H. J. Pullens, M. P. Schwartz, I. Broeders, and F. van der Heijden, "A real-time target tracking algorithm for a robotic flexible endoscopy platform," in *International Workshop on Computer-Assisted and Robotic Endoscopy*. Springer, 2015, pp. 81–89.

[14] N. van der Stap, C. H. Slump, I. A. Broeders, and F. van der Heijden, "Image-based navigation for a robotized flexible endoscope," in *International Workshop on Computer-Assisted and Robotic Endoscopy*. Springer, 2014, pp. 77–87.

[15] R. Reilink, G. de Bruin, M. Franken, M. A. Mariani, S. Misra, and S. Stramigioli, "Endoscopic camera control by head movements for thoracic surgery," in *Biomedical Robotics and Biomechatronics (BioRob), 2010 3rd IEEE RAS and EMBS International Conference on*. IEEE, 2010, pp. 510–515.

[16] M. Cianchetti and A. Menciassi, "Soft robots in surgery," in *Soft Robotics: Trends, Applications and Challenges*. Springer, 2017, pp. 75–85.

[17] J. Fraś, J. Czarnowski, M. Maciaś, J. Główka, M. Cianchetti, and A. Menciassi, "New stiff-flop module construction idea for improved actuation and sensing," in *2015 IEEE International Conference on Robotics and Automation (ICRA)*. IEEE, 2015, pp. 2901–2906.

[18] Y. Kim, S. S. Cheng, M. Diakite, R. P. Gullapalli, J. M. Simard, and J. P. Desai, "Toward the development of a flexible mesoscale mri-compatible neurosurgical continuum robot," *IEEE Transactions on Robotics*, vol. 33, no. 6, pp. 1386–1397, 2017.

[19] J. E. Bernth, A. Arezzo, and H. Liu, "A novel robotic meshworm with segment-bending anchoring for colonoscopy," *IEEE Robotics and Automation Letters*, vol. 2, no. 3, pp. 1718–1724, 2017.

[20] H. Naghibi, M. W. Gifari, W. Hoitzing, J. W. Lageveen, D. M. van As, S. Stramigioli, and M. Abayazid, "Development of a multi-level stiffness soft robotic module with force haptic feedback for endoscopic applications," in *2019 International Conference on Robotics and Automation (ICRA)*. IEEE, 2019, pp. 1527–1533.

[21] J. A. Lenssen, H. Naghibi, and M. Abayazid, "Evaluation of design aspects of modular pneumatic soft robotic endoscopes," in *2019 2nd IEEE International Conference on Soft Robotics (RoboSoft)*, Apr. 2019, pp. 56–61.

[22] K. Shoemake, "Animating rotation with quaternion curves," in *ACM SIGGRAPH computer graphics*, vol. 19, no. 3. ACM, 1985, pp. 245–254.

[23] J. Hilgert, K. Hirsch, T. Bertram, and M. Hiller, "Emergency path planning for autonomous vehicles using elastic band theory," in *Proceedings 2003 IEEE/ASME International Conference on Advanced Intelligent Mechatronics (AIM 2003)*, vol. 2. IEEE, 2003, pp. 1390–1395.

[24] J. Lenssen, "Towards a steerable multi-module soft robotic endoscope for NOTES applications," Master's thesis, University of Twente, Enschede, The Netherlands, June 2019.